Pimenteiras Shale: Characterization of an Atypical Unconventional Petroleum System, Parnaiba Basin, Brazil*

Frederico S. de Miranda[1]

Search and Discovery Article #10639 (2014)
Posted September 22, 2014

*Adapted from extended abstract prepared in conjunction with oral presentation given at AAPG International Conference & Exhibition, Istanbul, Turkey, September 14-17, 2014, AAPG © 2014. Please see closely related article, "Shale Gas/Oil: The New Frontier Exploration in Brazil", Search and Discovery article #10509.

[1]Parnaíba Gás Natural S.A., Rio de Janeiro, RJ, Brazil (frederico.miranda@pgnsa.com.br)

Abstract

The Parnaíba Basin is an intracratonic basin located in northeastern Brazil (Figure 1) and is one of the five Paleozoic basins in the country (Amazonas, Solimões, Paraná and Parecis basins). The basin covers an area of approximately 600,000 km² (231,661 mi²) and the sedimentary package can reach up to 3,500 m (11,735 ft) in the depocenter (Milani and Zalán, 1999). The sedimentary sequence is intruded by multiple sills that had a great impact on the petroleum system. Explored since the early 1950's the only significant discoveries in the basin were achieved in the 2000's. The OGX Maranhão, a subsidiary from OGX Petróleo e Gás S.A., declared commerciality of three gas fields with a total volume of gas in place ranging from 1.3 to 1.6 TCF. Now the owner and operator of these fields, including additional exploratory acreage is the Parnaíba Gás Natural S.A. The sandstones from the Late Devonian Cabeças Formation and the Mississippian Poti Formation are the main reservoirs for the conventional gas accumulations (OGX, 2012). The primary source rock is the Devonian Pimenteiras Formation (Figure 2), with secondary source rocks in the Silurian Tianguá Formation and the Early Carboniferous Longá Formation. The Cretaceous Codó Formation also has significant organic-rich intervals but besides its excellent geochemical characteristics it is usually found immature (Mendes, 2007). As reported by Cunha et al. (2012) all exploratory wells in the basin presented gas shows in the Pimenteiras Formation intervals. This leaded to research of the Pimenteiras Shale as a potential shale-gas play in the basin. Based on 48 sidewall core plugs from a wildcat well, wireline log suite, thin section descriptions, Source Rock Analyzer, SEM, and QEMScan data an integrated approach was conducted in order to provide an initial characterization of the Pimenteiras Shale.

Primenteiras Formation

The Pimenteiras Formation is more than 500 m (1640 ft) thick with TOC from 0.38% to 4.77%, but the highest TOCs are largely concentrated in three levels of the formation (Rodrigues, 1995) that can sum up to 70 m (230 ft). These are defined from bottom to top as A, B and C with Eifelian/Givetian (387 Ma), Givetian (387-382 Ma) and Frasnian ages (382-372 Ma), respectively (Rodrigues, 1995; Mello 2002). The average thicknesses are: A – 13 m (42 ft), B – 17 m (56 ft) and C – 40 m (131 ft). At the depocenter, the average burial depth of the Pimenteiras Formation today is 2000 m (6562 ft), and outcrops occur at the basin margins (Petersohn, 2007; Rodrigues, 1995). The Pimenteiras C interval

corresponds to the maximum flooding event in the overall transgressive cycle that lithostratigraphically corresponds to the lower and intermediate portions of the Pimenteiras Formation. The upper part of the Pimenteiras Formation and the lower part of the Cabeças Formation defines the following regressive cycle. Locally the upper contact of the Pimenteiras Formation with the Cabeças Formation is defined as an erosive surface (Della Fávera, 1990). The interbedded discontinuous sandstone bodies within the Pimenteiras Formation are defined as the Carolina Member (Carozzi, 1975) that can be the result of higher order forced regressions during the transgression (Young, 2006).

The Pimenteira Formation was deposited in a storm-dominated eperic sea with influence of deltaic systems. The major sediment source areas were located to the southeast, west and subordinately to the north. During Pimenteiras Formation deposition the Paranaiba Basin was connected in the northwest to the Amazonas/Solimões Basin and to the southwest to the Paraná Basin comprising a significant intracratonic sea. Regionally, the main facies are related to prodelta and upper offshore systems with subordinately delta front and bars complexes (Carozzi, 1975; Vaz et al., 2007).

The high resolution sequence stratigraphy (Young, 2006) at the eastern margin of the basin interpreted the Pimenteiras Formation as built by a succession of interbedded mudstones and sandstones intervals. This scenario greatly contributes to the quality of the self-sourced petroleum system, since the brittle facies are expected to be gas producible after stimulation. Similar facies from those recognized by Young (2006) were also identified in this study, in the central part of the basin.

The flooding event registered during the Parnaiba Basin's Devonian interval can be correlated with the Devonian seaway incursions in the U.S. and to the major Paleozoic's source rocks in South America and North Africa as well (Figure 3) (Scotese, 2003; Milani and Zalán, 1999).

The maturity of the organic-rich mudstones is closely related to the thermal effect of the sills that are widespread in the basin (Rodrigues, 1995). A similar hydrocarbon generation mechanism has been reported in several sedimentary basins worldwide such as the Paraná, Amazonas and Solimões basins in Brazil; the Neuquén Basin in Argentina; the Liahoe Basin in China; the Bight Basin and the Exmouth sub-basin in Australia; the Kerala-Konkan Basin in India; and the Karoo Basin in South Africa (Eiras and Wanderley Filho, 2009; Milani and Zalan, 1999; Rodriguez Monreal, 2009; Jackson, 2013; Mishra et al., 2008; Aarnes et al., 2010). Those can be defined as atypical petroleum systems according to Magoon and Dow (1994), where source rock maturity is achieved by influence of magmatic activity instead of overburden. The main characteristic of this atypical system (Magoon and Dow, 1994), in this case, is that the intrusion-related generation period occurs in a short time span. On the other hand, the overburden process of maturation occurs when the source rocks are exposed to relatively lower temperatures during a long period of time (North, 1985).

The Early Jurassic and Early Cretaceous sills are commonly found within the Pimenteiras Formation (Vaz et al., 2003). The main impacts of the igneous intrusions were: (i) increase in the geothermal gradient providing intense heat for hydrocarbon generation during a short period of time; (ii) doming and uplift of the overlain layers; and (iii) creation of a contact metamorphism rim in the host rocks. As the main source rock for the basin (Rodrigues, 1995), the Pimenteiras Formation has the greatest potential for unconventional resources as an atypical self-sourced shale-gas system.

Microfacies Characterization

The Pimenteiras Shale can be petrographically subdivided into eight microfacies, as shown in Table 1, Figure 2 and Figure 4. The defined microfacies are thinly interbedded and are related to turbidity currents, storm-wave reworking and bottom currents. Four depositional environments are recognized based on the sedimentary structures and trace fossils. Those are: (i) wave-influenced delta front, (ii) prodelta, (iii) upper offshore, and (iv) transgressive lag. Due to the complete recrystallization of the matrix the siliciclastic hornfels were not encompassed in any environment. The bioturbation index (BI) was reported for each sample following previous works (Reineck, 1967; Taylor and Goldring, 1993; Bann et al., 2004; Dafoe et. al., 2010). Unbioturbated samples have a BI equal to 0, sparsely burrowed BI 1, low degree of burrowing BI 2, moderately burrowed BI 3, commonly burrowed BI 4, abundant burrowing BI 5 and pervasive burrowing BI 6.

Wave Influenced Delta Front

The wave influenced delta front reflects the higher energy deposits in the Pimenteiras Shale succession with higher quartz content, low organic carbon, abundant wave ripples, pyrite lags and organic matter fragments. No bioturbation was observed in this facies (BI 0). The increase in clay content from facies A (Muddy Sandstone) to facies B (Muddy sandstone couplets) is interpreted as a response to the reduction in energy environment related to periods of quiescence and lower sedimentation rate allowing the deposition and preservation of the mud-rich laminas. Traces of siderite and the organic matter fragments are associated with riverine discharge in the delta system context. Based on four sidewall core samples the average TOC for wave influenced delta front facies is 1.36%, with quartz content of 45% and clay content 50%.

Prodelta

The increase of mud and reduction of the quartz content observed in this facies are interpreted as a more basinward position in the Pimenteiras Shale succession. The prodelta is composed by Facies C (sandy-mudstone couplets), Facies D (bioturbated mudstone couplets), and Facies E (laminated claystone). These are the more abundant facies described in this study and are believed to be the most recurrent facies in the Pimenteiras Shale. Increase in bioturbation index from BI 0 to BI 4 is characteristic from facies C to D, respectively. Synaeresis crack and traces of siderite are interpreted as the influence of the riverine discharge in the prodelta settings. The identified trace fossils are defined by structures from dwelling (*Palaeophycus, Skolithos*), deposit-feeding (*Teichichnus, Rhizocorallium,* and *Thalassinoides*), and grazing behaviors (*Helminthopsis*). The present ichnofossil assemblage would represent a subtly stressed expression of the Distal Cruziana ichnofacies. Turbidity currents of a lower sedimentation rate and more oxic conditions allowed the colonization of the substrate observed in Facies D. Based on thirty-five sidewall core samples, the average TOC for prodelta facies is 1.17%, with quartz content 26% and clay content 73%.

The upper offshore is represented by Facies F (organic rich mudstones). An increase in total organic carbon and the pyrite content with the lack of trace fossils (BI 0) are diagnostic of this facies. These features suggest that anoxic conditions and lower sedimentation rates were present during deposition. It is believed the upper offshore facies define the main source rocks in the Pimenteiras Shale succession and is likely to be related to flooding surfaces. Based on three sidewall core samples, the average TOC for upper offshore facies is 4%, with quartz content 30% and clay content 70%.

Transgressive Lags

This facies association is represented by the Facies G – Chaotic muddy-sandstone. The poorly sorted sediments, lack of preserved sedimentary structures, BI 4 to 5 and the relationship to a sedimentation turning point observed in the wireline logs suggests the interpretation of a transgressive surface of erosion associate to these facies. The recognized trace fossils are related to dwelling (*Palaeophycus*) and grazing (*Helminthopsis*) structures. Further ichnological work is required to identify the diverse assemblage present in this facies.

Contact Metamorphism

Towards the proximity of the sills the sedimentary structure is severely obliterated due to the contact metamorphism. A complete recrystallization of the mineral matrix and the nucleation of new mineral phases is observed in one sample that defines Facies H (siliciclastic hornfels). The QEMScan data showed a quartz nodule, surrounding albite, chlorite, illite and muscovite matrix. A faint plane parallel lamination can still be observed, but this could be a product of the recrystallization. The thermal effect of the intrusion was responsible for overcooking any available organic carbon in this facies. The TOC for Facies H is 0.14%, with quartz 35% and clay content 65%.

Facies Analysis

The QEMScan® data was incorporated to the thin section descriptions in order to provide a better understanding of the composition of the fine grained rocks. The TOC values obtained in the Source Rock Analyzer were also relevant to interpret environment of deposition, specifically in terms of source rock potential, ox-redox conditions and system energy. The SEM and BSE observations on the micrometer and nanometer scale were also incorporated in order to assess the full range of rock texture.

Geochemistry

The forty eight available sidewall core plugs were submitted to the Source Rock Analyzer at the Colorado School of Mines, while one sample was submitted to the TerraTek laboratory at Salt Lake City for organic petrology and vitrinite reflectance measurement. TOC values range from 0.36% to 4.77%, which is inversely proportional to the quartz content and directly proportional to the pyrite content. TOC values greater than 3% are only found in samples with average quartz content lower than 40%. The remaining potential of the source rocks (S2) is low, below 1 mg of HC/g of rock. The hydrogen indexes are also low, ranging from 6 to 50 mg of HC/g of Carbon. This effect has been previously reported in the basin and is related to the thermal effect of the sills (Rodrigues, 1995). The same effect resulted in unreliable values of Tmax which leaded to incoherent values of the calculated vitrinite reflectance (Jarvie, 2007). The positive correlation between TOC and gas shows suggests that part of the generated hydrocarbons are still stored in the source rocks.

The Van-krevelen diagram (Figure 5) shows a possible thermal evolution of the types II and III kerogen found in the Pimenteiras Shale compared with the available data for the basin (Rodrigues, 1995). It was expected that the heat provided by the sills would be the major cause for the hydrocarbon generation and resulted in the Type IV kerogen signature observed in the studied samples. Based on the sill thicknesses and distance from the sample a relative distance from the sill was used to calculate the thermal maturity, according to Rodrigues (1995). One

Ro laboratory measurement was added to an estimation of the vitrinite reflectance, slightly adjusting the curve to the study well (Figure 6). Considering this calculation in the distance up to 110% of the sill thickness, we would expect to find the source rocks in the gas generation window. In distances between 110% and 240% of the sill thickness we would expect to find the source rocks in the oil generation window.

Nanofabric

Six samples from Facies D, E, and F were prepared and analyzed using a high resolution SEM (up to 100,000x magnification). The samples were ion-milled in order to obtain a smooth surface for appropriate textural analysis. To acquire a wider image of the nanofabric of the samples a photomosaic was created for each sample. The images were acquired using the backscattered electron detector (BSED) and a 3,000 times magnification. Seventy 85 x 100 μm individual pictures were stitched resulting in a 490 x 795 μm mosaic. Three samples of Facies D (Bioturbated sandy-mudstone couplets), one sample of Facies E (Laminated Claystone), and two samples of Facies F (Organic rich mudstone) were examined.

The sample 6, Facies E, exhibit a strong plane-parallel orientation of the clay flakes and organic matter. Differential compaction is observed around silt size quartz grains, pyrite framboids and clay aggregates. Locally, bioturbation is responsible for the reorientation of the clay flakes. Organic matter is elongated and amorphous commonly associated with pyrite. Intraplatellet porosity and semi-filled fracture porosity were observed. No organic porosity occurs in the sample (Figure 7). The relative distance of the main sill is 277% and estimated Ro of 0.58%.

The sample 20 Facies D contains a less oriented microfabric related to the coarser grained fraction (Figure 8). Organic matter occurs as blocky particles and as elongated amorphous material. Pyrite occurs as euhedral crystals and framboids. The porosity is intergranular or intraplatellet. The organic matter does not exhibit porosity. The relative distance from the sill is 269.5% and the estimated Ro are 0.68%. Samples 33 and 38, also belonging to Facies D, are a relative distance to the sill of 190.5% and 140.5% with estimated Ro of 0.93% and 1.17%, both in the oil window. These samples, closer to the main sill, contain organo-pores in spongy and spider-web pore geometry. Anhydrite semi-filled fractures are also present sub-parallel to the lamination. Bioturbation is responsible for the reorientation of the rock fabric and could possibly enhance permeability.

The samples 43 and 46 from Facies F contain a plane-parallel oriented fabric with abundant pyrite framboids (Figure 9). Those often present intercrystalline porosity. Organo-pores are well developed with a spongy texture. Some organic matter grains do not exhibit porosity which is believed to be related to type III kerogen. Intraplatellet porosity also occurs. Quartz recrystallization is common and is more frequent closer to the sill. The relative distances to the sill are 91% and 80% with respectively estimated Ro of 1.55% and 1.76%, already in the gas window.

Composition

Based on the QEMScan® analysis the studied interval is clay-rich with an average normalized composition of 40% quartz and 60% clay (Figure 10). Compared to several U.S. shale plays it is clear that the high clay content will be a challenge for the hydraulic fracturing stimulation. The presence of interbedded quartz-rich facies, such as Facies A and Facies G, among the organic rich intervals represented by Facies F can be considered an upside for the play. The storm influence events, resulting in tempestite bedding, is observed where there is an

enrichment in quartz content at the base of the lamina set which fine-upwards to higher clay content laminas (Figrue 11). Bioturbation was identified as a texture and mineralogy-transforming agent (Figure 11), whereas organism mucus can act as a nucleation site for diagenetic minerals crystallization (Buatois and Mángano, 2011).

Log Response

Based on standard equations (Zoback, 2007) the Compressional and Shear sonic data were used to calculate the dynamic mechanical properties and further converted to static properties (Dvorkin, 2001) of the study interval. Based on a hydrostatic gradient of 8.45 lb/gal, sonic slowness normal compaction trend, density log integer and the Eaton's Equation (Eaton, 1975) the pressure gradient versus depth plot was constructed. An overpressured interval is recognized and associated with the organic rich facies of the Pimenteiras Shale. Gas saturated intervals are coincident with the overpressured compartment and higher TOC. The log derived TOC was based on Passey delta-log-R (Passey et al., 1990) technique and uranium content, calibrated to the sidewall core measurements (Figure 12).

Conclusions

The Devonian Pimenteiras Shale is the main source rock for the conventional and unconventional petroleum systems in the Parnaíba Basin. The fine-grained succession was divided into eight main microfacies related to wave influenced delta front, prodelta, upper offshore, transgressive lags, and contact metamorphism aureole. In the study well the TOC varies from 0.38% to 4.77% with type IV signature due to overcooking by the sills. Preserved samples geochemistry defines a type II and III signature for kerogen (Rodrigues, 1995). The relative distance from the sill is the major control on thermal maturity, expressed by the calculated vitrinite reflectance. Diverse pore types are present in the analyzed samples, including organo-pores, clay intraplatellet porosity, intercrystalline porosity and fracture porosity. The high clay content is challenging but the interbedded nature of quartz-rich and clay-rich facies, such as Facies A and Facies F, respectively, could be a positive aspect. The more brittle facies are recommended to be targeted for horizontal drilling and multi-stage hydraulic fracture stimulation.

The gas shows in all the drilled wells in the Pimenteiras Shale, the good TOC content and presence of an effective porosity system confirms the existence of a self-sourced atypical unconventional petroleum system. For future studies we recommend the use of geomechanical data from core and adsorption isotherms in order to design the hydraulic fracture stimulation and estimate the original gas-in-place.

References Cited

Aarnes, I., H. Svensen, S. Polteau, and S. Planke, 2011, Contact metamorphic devolatilization of shales in the Karoo Basin, South Africa, and the effects of multiple sill intrusions: Chemical Geology, v. 281/3, p. 181-194.

Bann, K.L., and C.R. Fielding, 2004, An integrated ichnological and sedimentological comparison of non-deltaic shoreface and subaqueous delta deposits in Permian reservoir units of Australia, *in* D. McIlroy, ed., The Application of Ichnology to Palaeoenvironmental and Stratigraphic Analysis: Geological Society, London, Special Publication 228, p. 273-310.

Bizzi, et al., 2003, Geologia, tectônica e recursos minerais do Brasil: texto, mapas & SIG, Brasília: CPRM – Serviço Geológico do Brasil, 692 p. ISBN 85-7499-006-X.

Buatois, L.A., and M.G. Mángano, 2011, Ichnology: Organism-substrate interactions in space and time: Cambridge University Press.

Carozzi, V.C., et al., 1975, Análise ambiental e evolução tectônica sinsedimentar da seção siluro-eocarbonífera da bacia do Maranhão. Rio de Janeiro, Petrobras, 2v.

Cunha, P.R.C., A. Bianchini, J.L. Caldeira, and C.C. Martins, 2012, Parnaíba Basin – The Awakening of a Giant: 11th Simposio Bolivariano-Exploracion Petrolera en las Cuencas Subandinas.

Dafoe, L.T., M.K. Gingras, and S.G. Pemberton, 2010, Wave-influenced deltaic sandstone bodies and offshore deposits in the Viking Formation, Hamilton Lake area, south-central Alberta, Canada: Bulletin of Canadian Petroleum Geology, v. 58/2, p. 173-201.

Della Fávera, J.C., 1990, Tempestitos na Bacia do Parnaíba: Tese de Doutorado, Universidade Federal do Rio Grande do Sul, Porto Alegre, 560 p.

Dvorkin, J., A.I. Mese, and M. Soliman, 2001, Disposal of drill cuttings; determining the properties of unconsolidated sandstones and clayey sands: Proceedings - Symposium on Rock Mechanics, p. 129-132.

Eaton, B.A., 1975, The equation for geopressure prediction from well logs, Fall Meeting of the Society of Petroleum Engineers of AIME: Society of Petroleum Engineers.

Eiras, J.F., and J.R. Wanderley Filho, 2003, Sistemas petrolíferos ígneo-sedimentares: Congresso Brasileiro de P&D em Petróleo & Gás, 2, Rio de Janeiro. Resumos.

Jackson, C.A-L., 2013, The Impact of Igneous Intrusions and Extrusions on Hydrocarbon Prospectivity in Extensional Settings: A 3D Seismic Perspective: Adapted from AAPG Distinguished Lecture, 2012-2013 Lecture Series.

Jarvie, D.M., R.J. Hill, T.E. Ruble, and R.M. Pollastro, 2007, Unconventional shale-gas systems: The Mississippian Barnett Shale of north-central Texas as one model for thermogenic shale-gas assessment: AAPG bulletin, v. 91/4, p. 475-499.

Magoon, L.B., and W.G. Dow, 1994, The petroleum system - From source to trap: AAPG Memoir 60, p. 3-24.

Melo, J.H.G., 2002, Revisão da biocronoestratigrafia de miósporos do Devoniano – Carbonífero Inferior da bacia do Amazonas e correlação com outras bacias paleozóicas brasileiras, Tese de Doutorado, IGEO-UFRJ, Rio de Janeiro, 103 p.

Mendes, M.S., 2007, Análise estratigráfica do intervalo formacional Grajaú–Codó (Aptiano) da bacia do Parnaíba, NE do Brasil, Programa de Pós-graduação em Geologia, Universidade Federal do Rio de Janeiro, Dissertação de Mestrado, 164 p.

Milani, E.J., and P.V. Zalan, 1999, An outline of the geology and petroleum systems of the Paleozoic interior basins of South America: Episodes, v. 22/3, p. 199-205.

Mishra, S., R. Verma, K. D'Silve, S. Banerjee, R. Bastia, and D.M. Nathaniel, 2011, Sub-Basalt Hydrocarbon Prospectivity in Kerala-Konkan Offshore Basin, India: A Basin Modeling Approach, Adapted from extended abstract presented at GEO-India, Greater Noida, New Delhi, India, January 12-14.

North, F.K., 1985, Petroleum geology (p. 607), Boston: Allen & Unwin.

Passey, Q.R., S. Creaney, J.B. Kulla, F.J. Moretti, and J.D. Stroud, 1990, A practical model for organic richness from porosity and resistivity logs: AAPG bulletin, v. 74/12, p. 1777-1794.

Petersohn, E., 2007, Brazil Round 09, Parnaíba Basin: Agencia Nacional do Petroleo, Gas Natural e Biocombustiveis, Bid Areas Department, 39 p.

Reineck, H.E., 1967, Parameter von Schichtung und Bioturbation. Geologische Rundschau, v. 56, p. 420-438.

Rodrigues, R.A., 1995, Geoquímica Orgânica na bacia do Parnaíba, 225 p., Tese (Doutorado em Geoquímica), Curso de Pós-Graduação em Geociências, Instituto de Geociências, Universidade Federal do Rio Grande do Sul, Porto Alegre.

Rodriguez Monreal, F., H.J. Villar, R. Baudino, D. Delpino, and S. Zencich, 2009, Modeling an atypical petroleum system: a case study of hydrocarbon generation, migration and accumulation related to igneous intrusions in the Neuquen Basin, Argentina: Marine and Petroleum Geology, v. 26/4, p. 590-605.

Scotese, C.R., 2003, Paleomap Project, University of Texas, Arlington. Website accessed September 10, 2014. http://www.scotese.com/moremaps2.htm

Taylor, A.M., and R. Goldring, 1993, Description and analysis of bioturbation and ichnofabric: Journal of the Geological Society, London, v. 150, p. 141-148.

Vaz, P.T., N.G.A. Mata Rezende, J.R. Wanderley Filho, and W.A.S. Travassos, 2007, Bacia do Parnaíba, Boletim de Geociências da Petrobrás, v. 15/2, p. 253-263.

Young, C., 2006, Estratigrafia de alta resolução da Formação Pimeteira (Devoniano, bacia do Parnaíba) 174 p. Dissertação (Mestrado em Paleontologia e Estratigrafia) - Programa de Pós Graduação em Geociências, Universidade Federal do Rio de Janeiro, Rio de Janeiro.

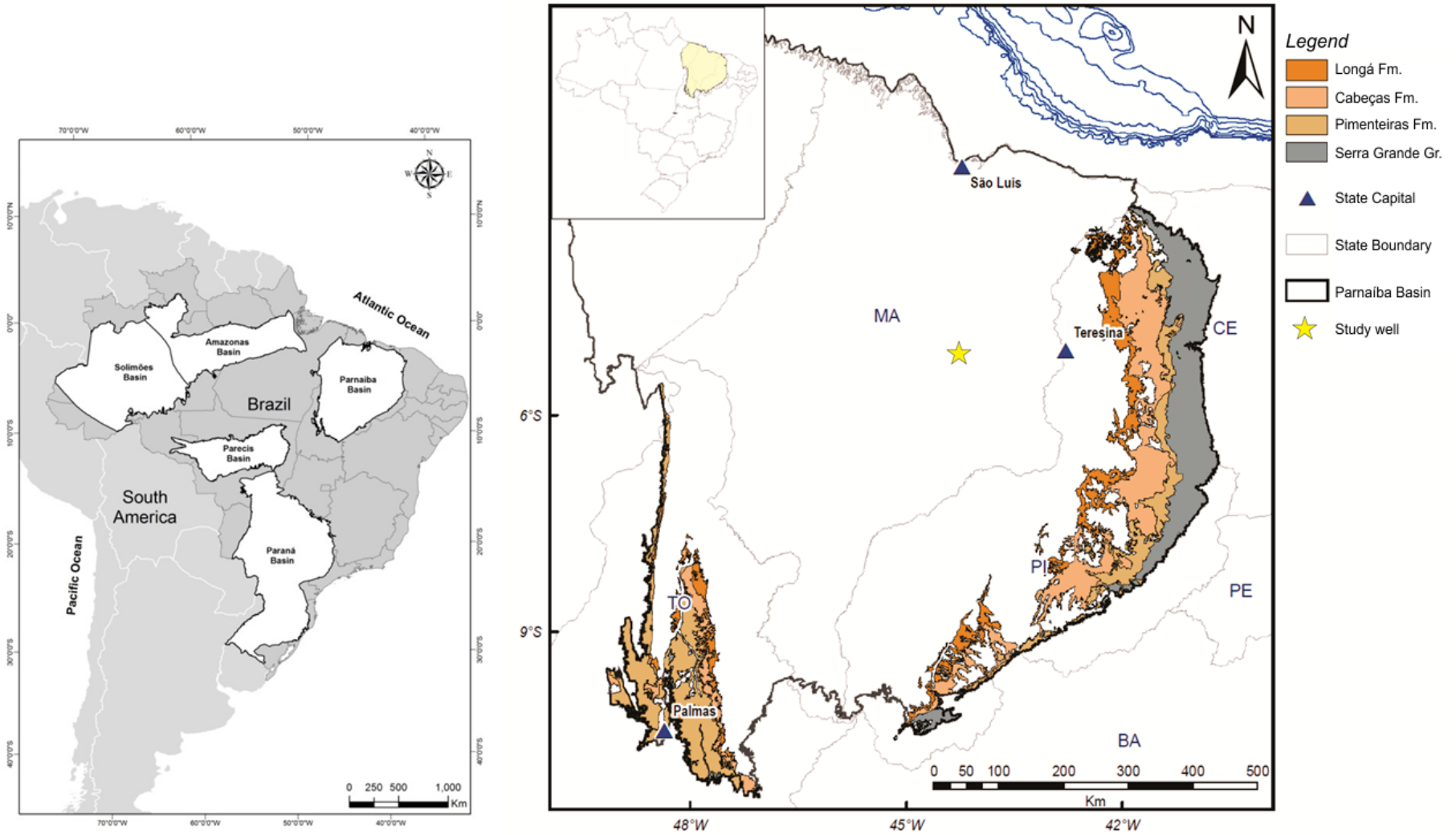

Figure 1. Location of the Paleozoic basins in Brazil. The Parnaíba Basin is located in northeastern Brazil (BR). The Pimenteira Formation outcorps at the eastern and southwestern margins of the basin. Modified from (Bizzi et al., 2003).

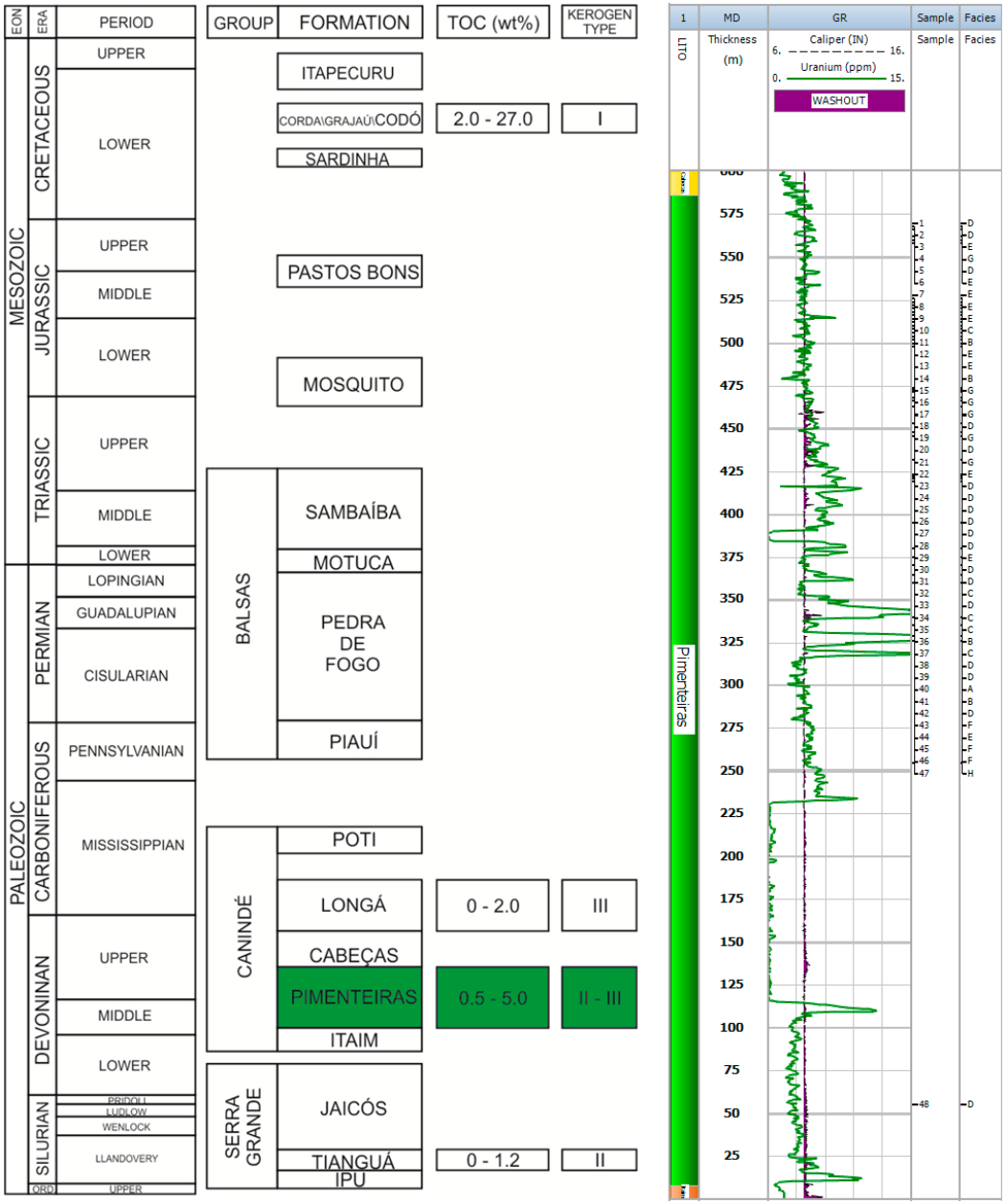

Figure 2. Schematic stratigraphic chart for the Parnaíba Basin. Total Organic Carbon and Kerogen Types are present for the source rocks intervals (Rodrigues, 1995; Mendes, 2006). Wireline log from the studied interval with samples location and facies. Thickness in meters.

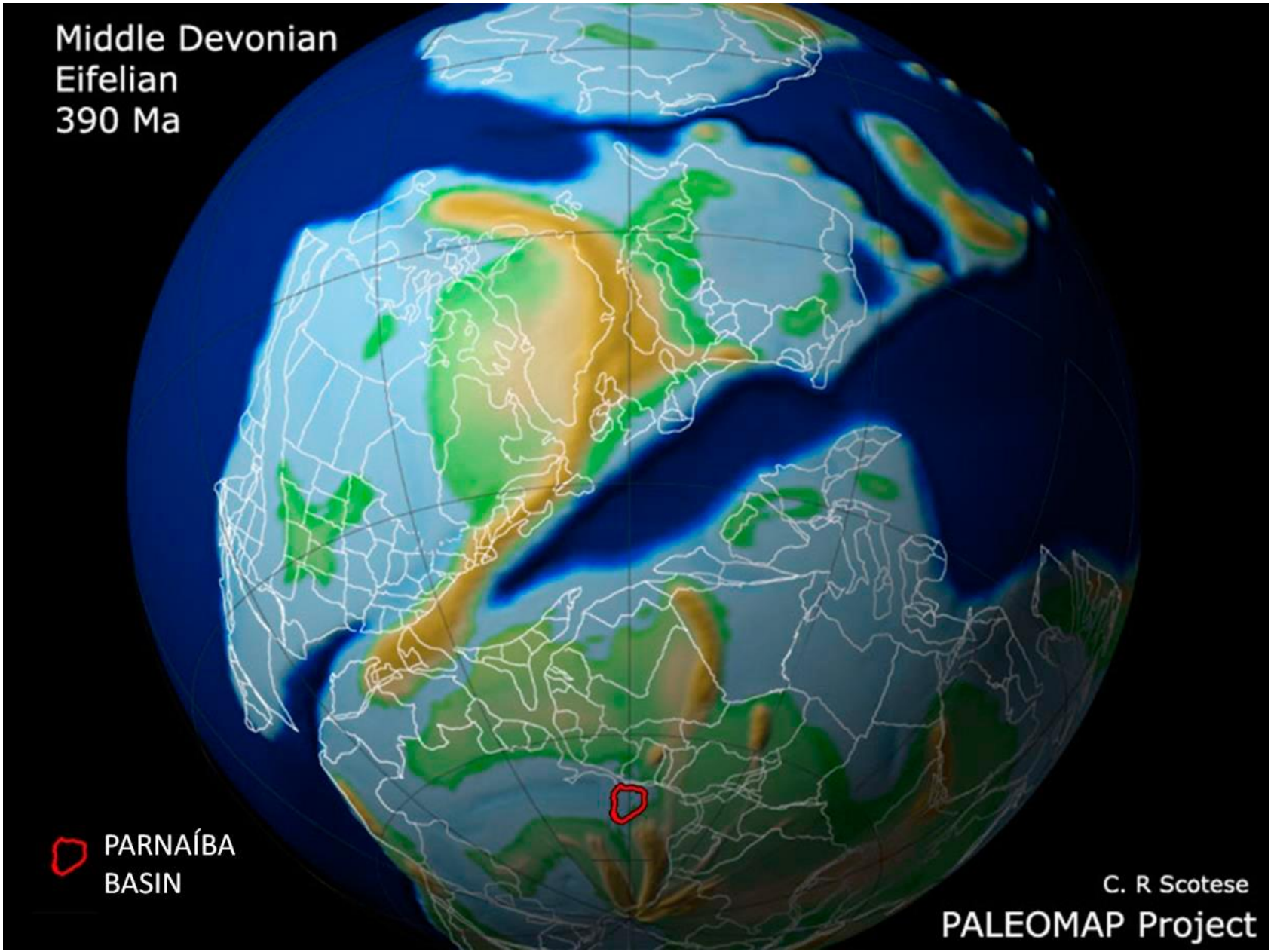

Figure 3. Paleogeographic map reconstruction of the Middle Devonian. The flooding event represented by the lower Pimenteiras Formation corresponds to a global transgression with source rock intervals in South America, North America and Africa (modified from Scotese, 2003).

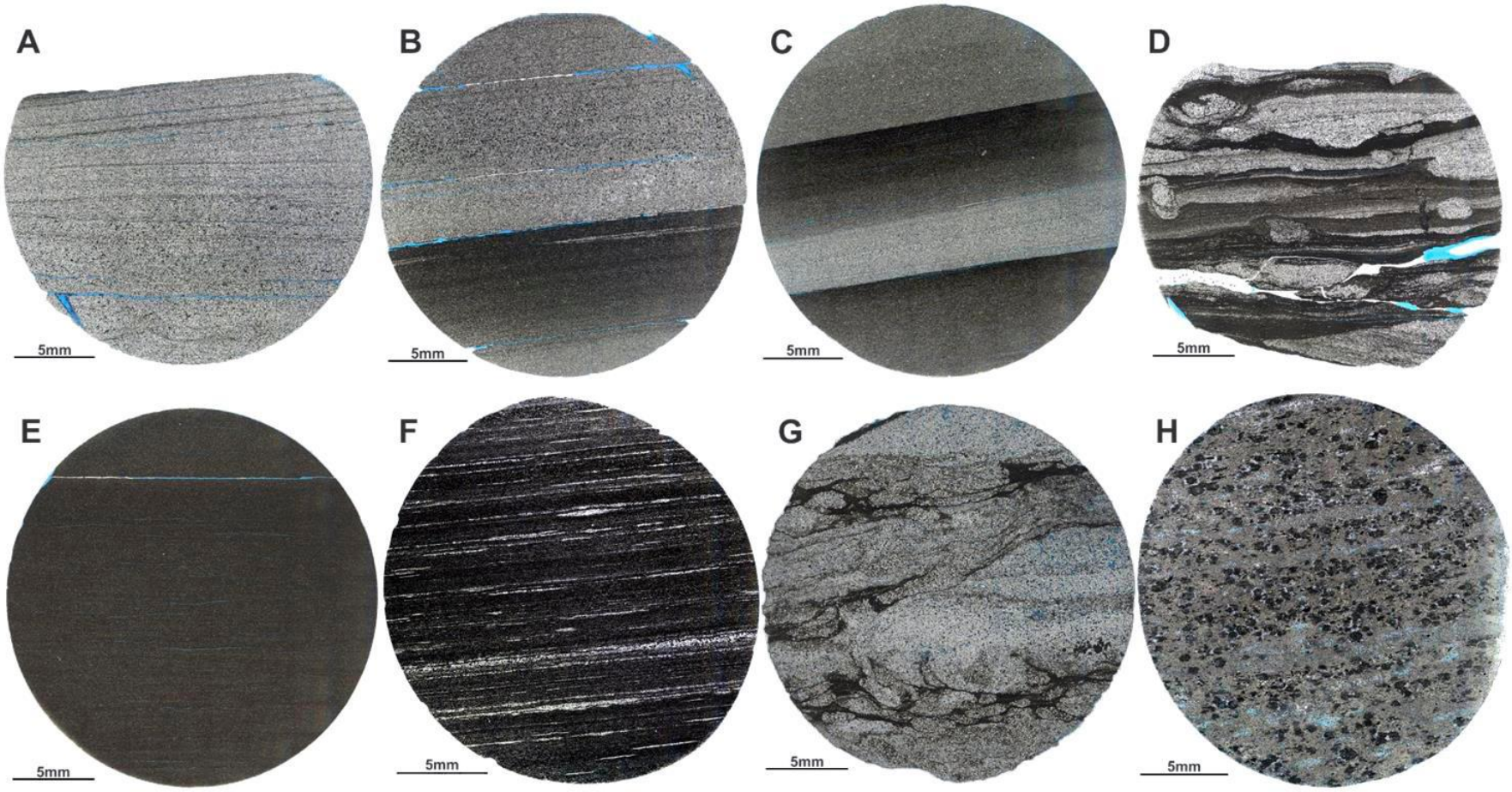

Figure 4. Thin section photographs of the eight identified microfacies in the Pimenteiras Shale succession: (A) muddy-sandstone, (B) muddy-sandstone couplets, (C) sandy-mudstone couplets, (D) bioturbated sandy-mudstone couplets, (E) laminated claystone; (F) organic-rich mudstone; (G) chaotic muddy-sandstone, and (H) siliciclastic hornfels.

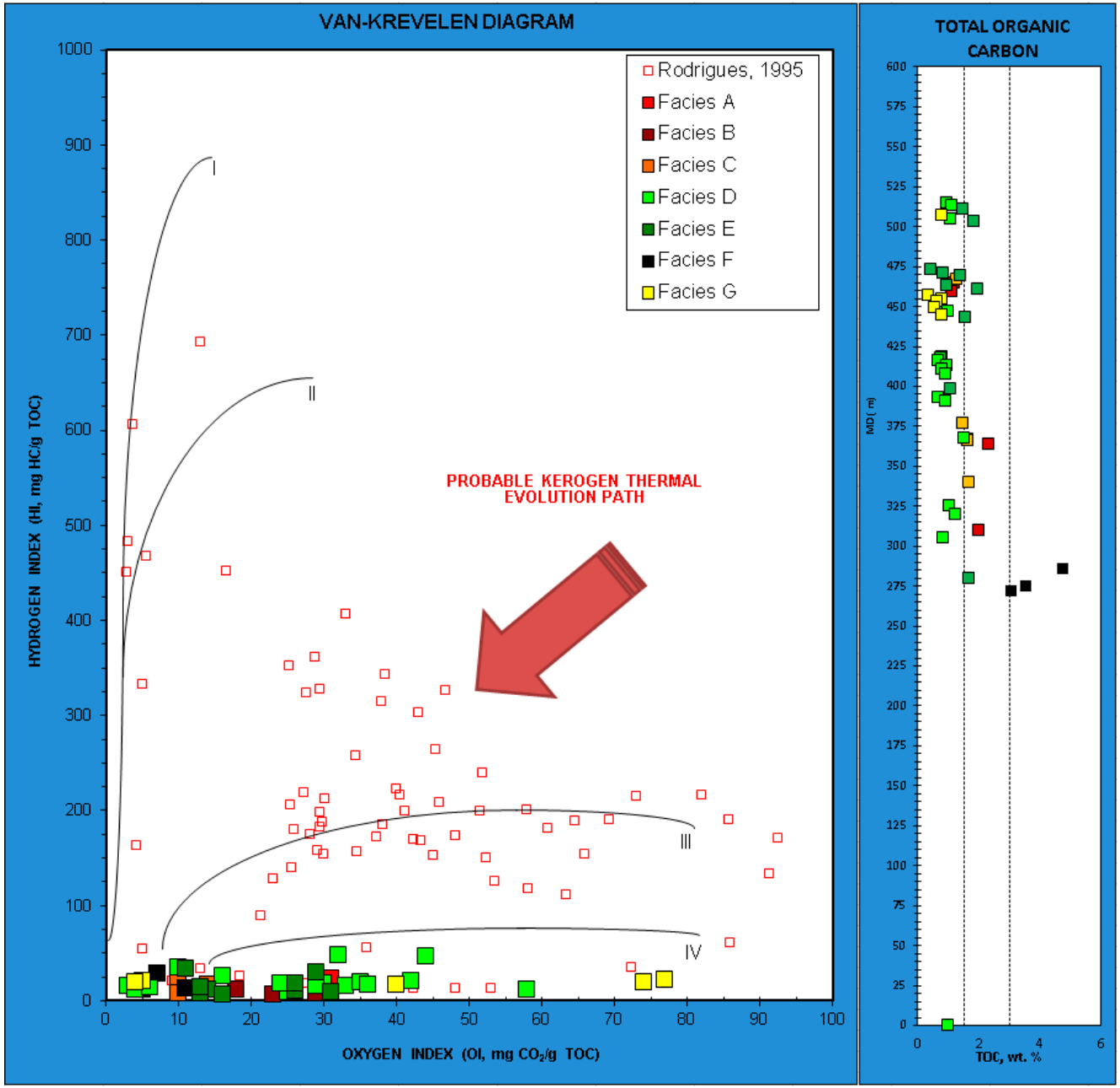

Figure 5. Van-krevlen diagram and TOC values for the 48 analyzed side-wall cores from the Pimenteira Shale.

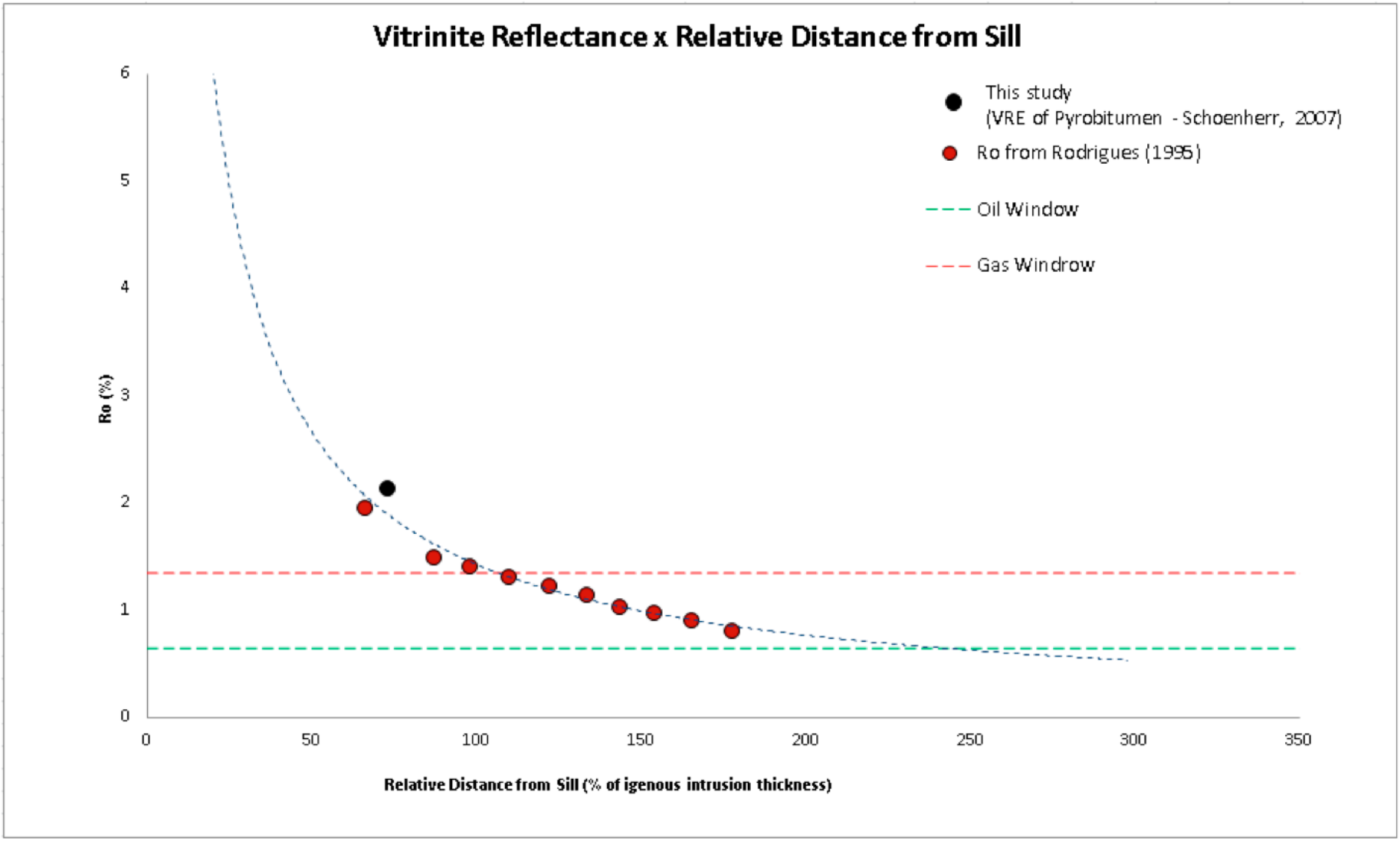

Figure 6. Estimated vitrinite reflectance versus relative distance from the sill.

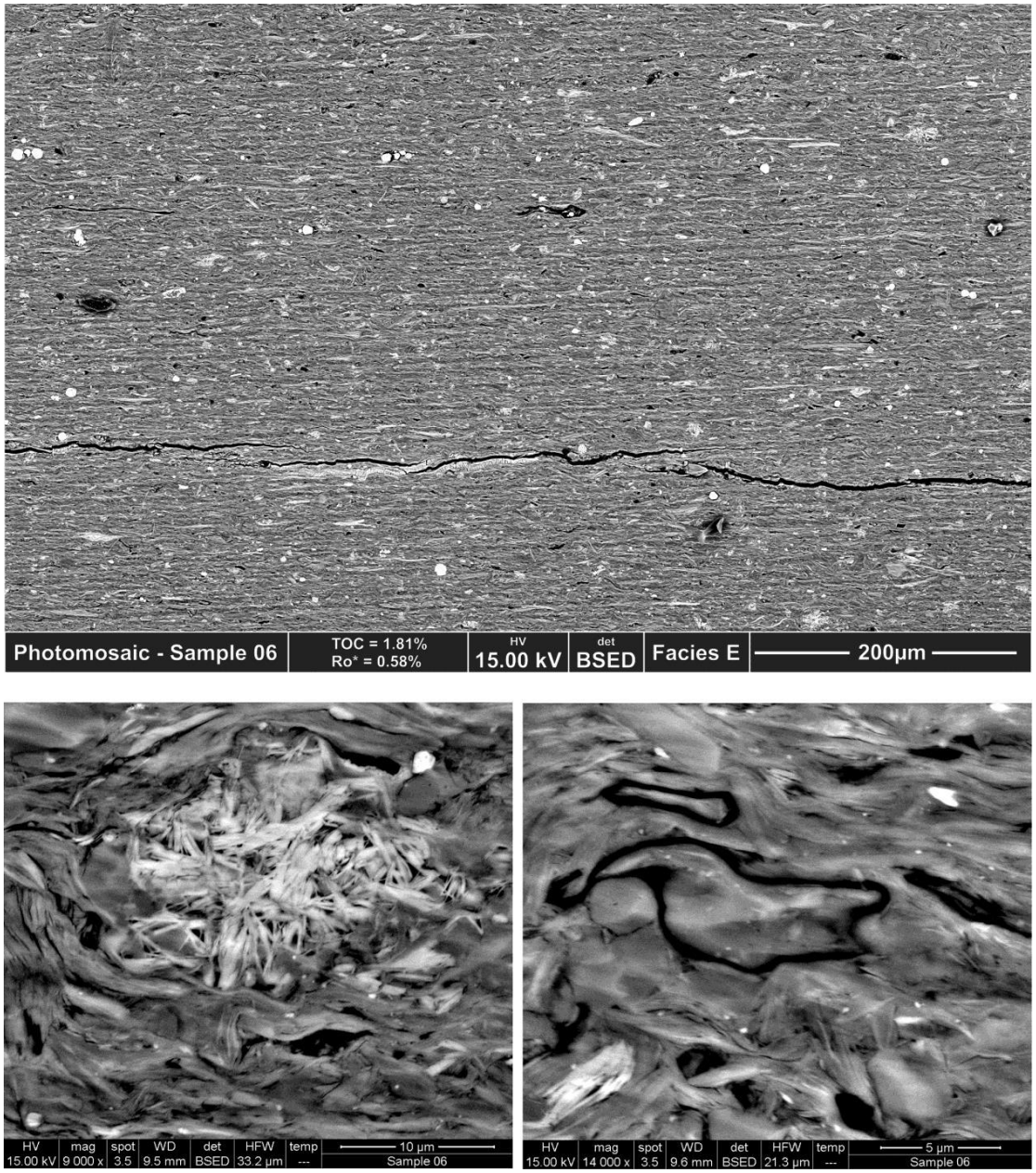

Figure 7. BSED mosaic from sample 06, representing facies E sharp tabular, continuous planar laminated, fining-upward, gutter-cast, claystone. No organo-pore was observed. *Bottom left:* clay aggregate intraplatellet porosity. *Bottom right:* amorphous organic matter.

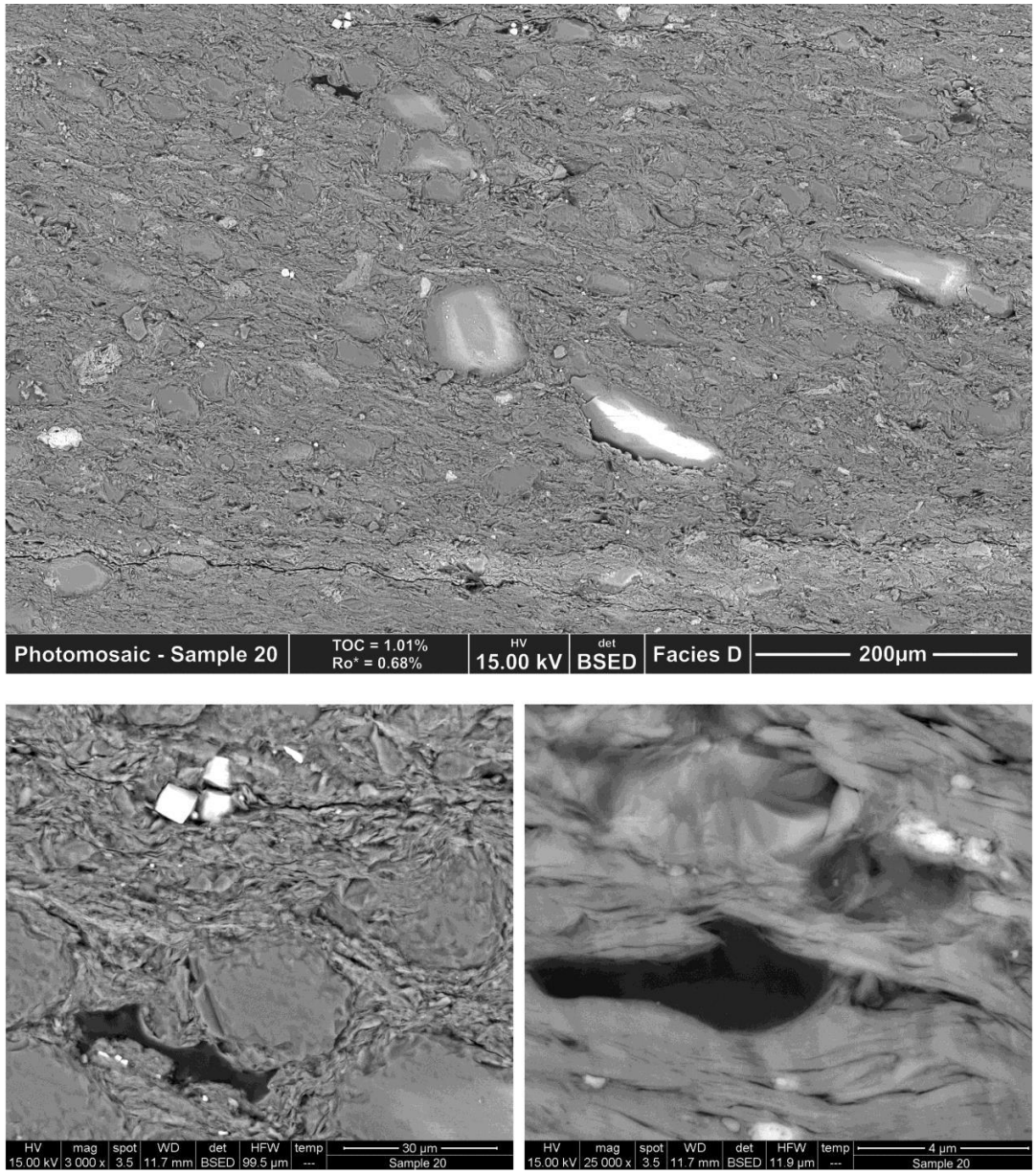

Figure 8. BSED mosaic from sample 20, representing facies D, burrowed concave-up and down, continuous planar to wavy laminated, lenticular, micaceous, fining-up, sandy mudstone. *Bottom left:* disorganized nanofabric associated with bioturbation, amorphous organic matter and intercrystalline porosity between pyrite crystals. *Bottom right:* amorphous organic matter without porosity and oriented clays.

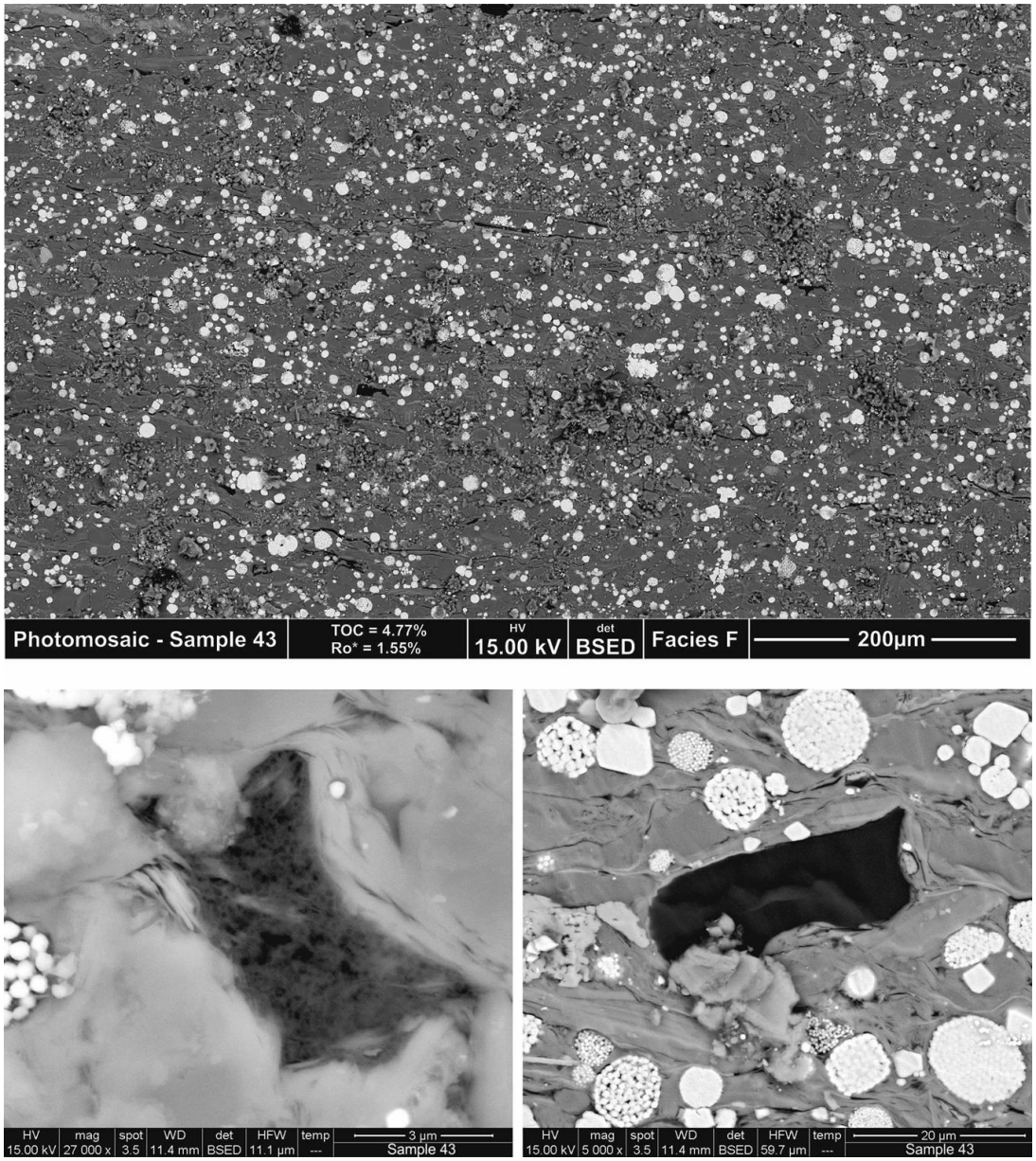

Figure 9. BSED mosaic from sample 43, representing facies F, non-bioturbated sharp tabular bedded plane-parallel laminated organic rich mudstone. *Bottom left:* amorphous organic matter with abundant organo-pores, intercrystalline porosity in pyrite framboids. *Bottom right:* non-porous amorphous organic matter and abundant pyrite framboids.

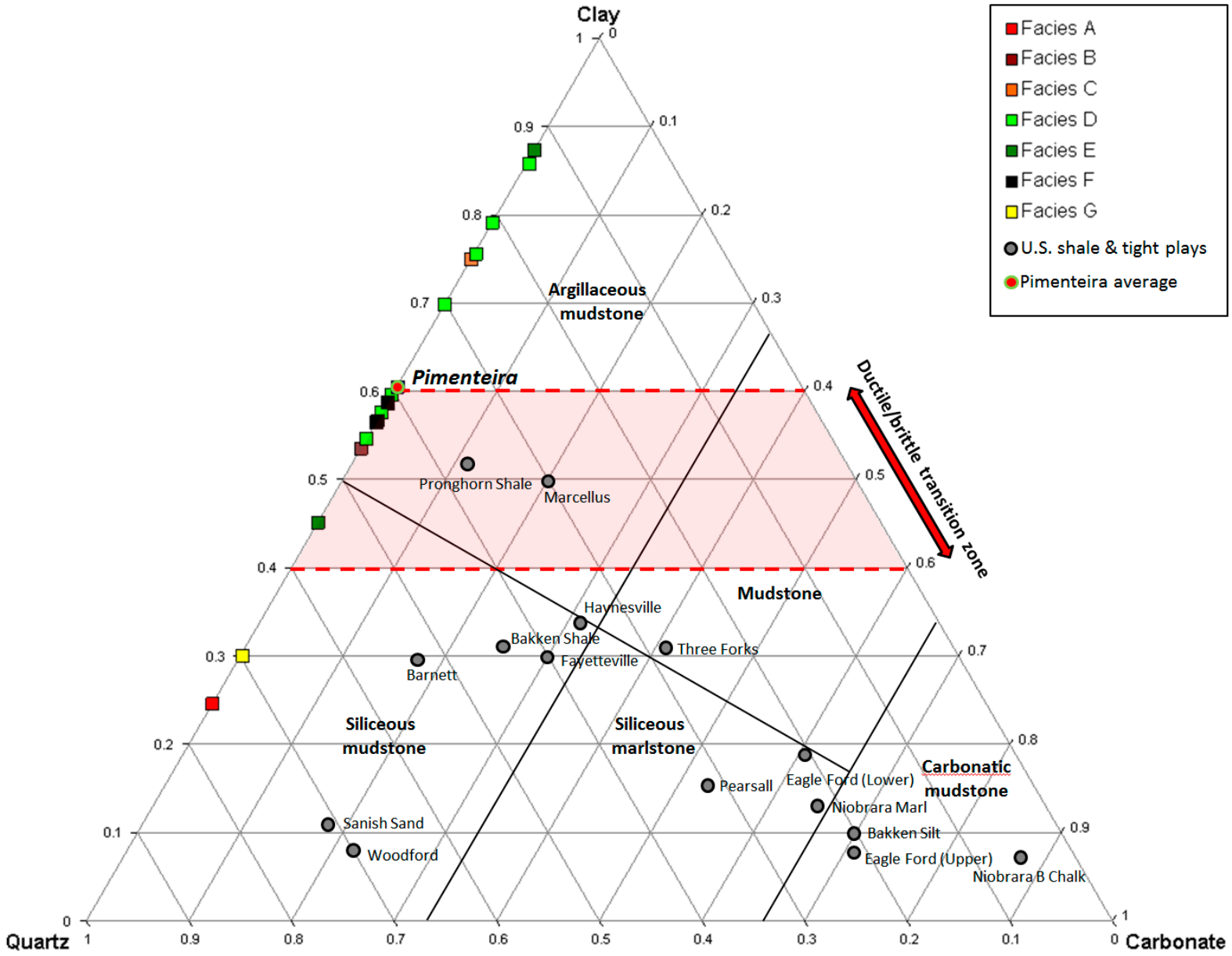

Figure 10. QEMSCan® compositional ternary plot of the Pimenteiras Formation analyzed samples and some major U.S. shale and tight reservoir plays (modified from Anderson, 2014).

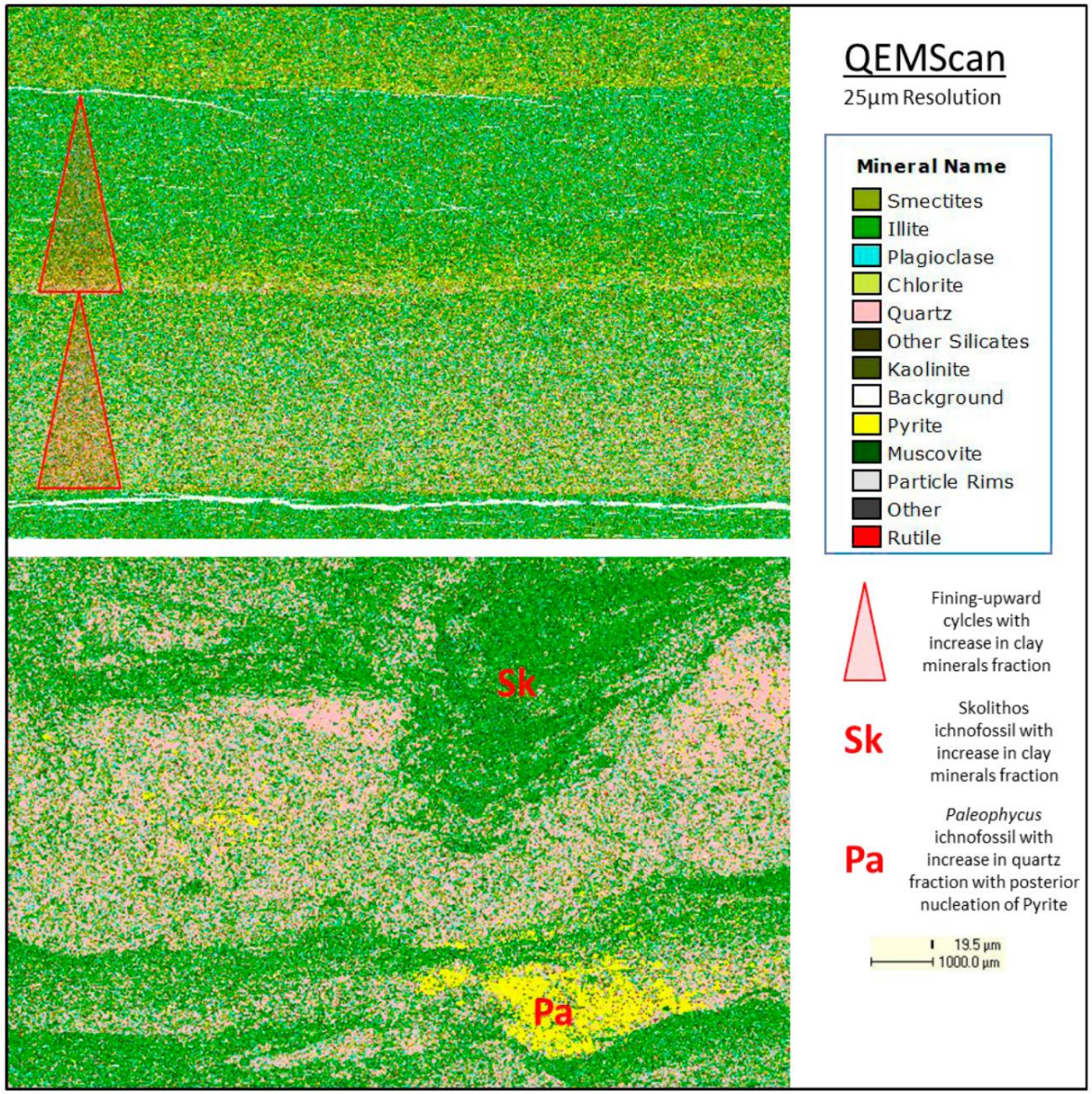

Figure 11. QEMScan images from facies C (top) and D (bottom). The tempestite bedding can be observed by the enrichment in the quartz content at the base of the lamina set with finning-upwards followed by the increase in the clay content in the mudstone couplets. Bioturbation was identified as a texture and mineralogy transforming agent, whereas organism mucus can act as a nucleation site for diagenetic minerals crystallization.

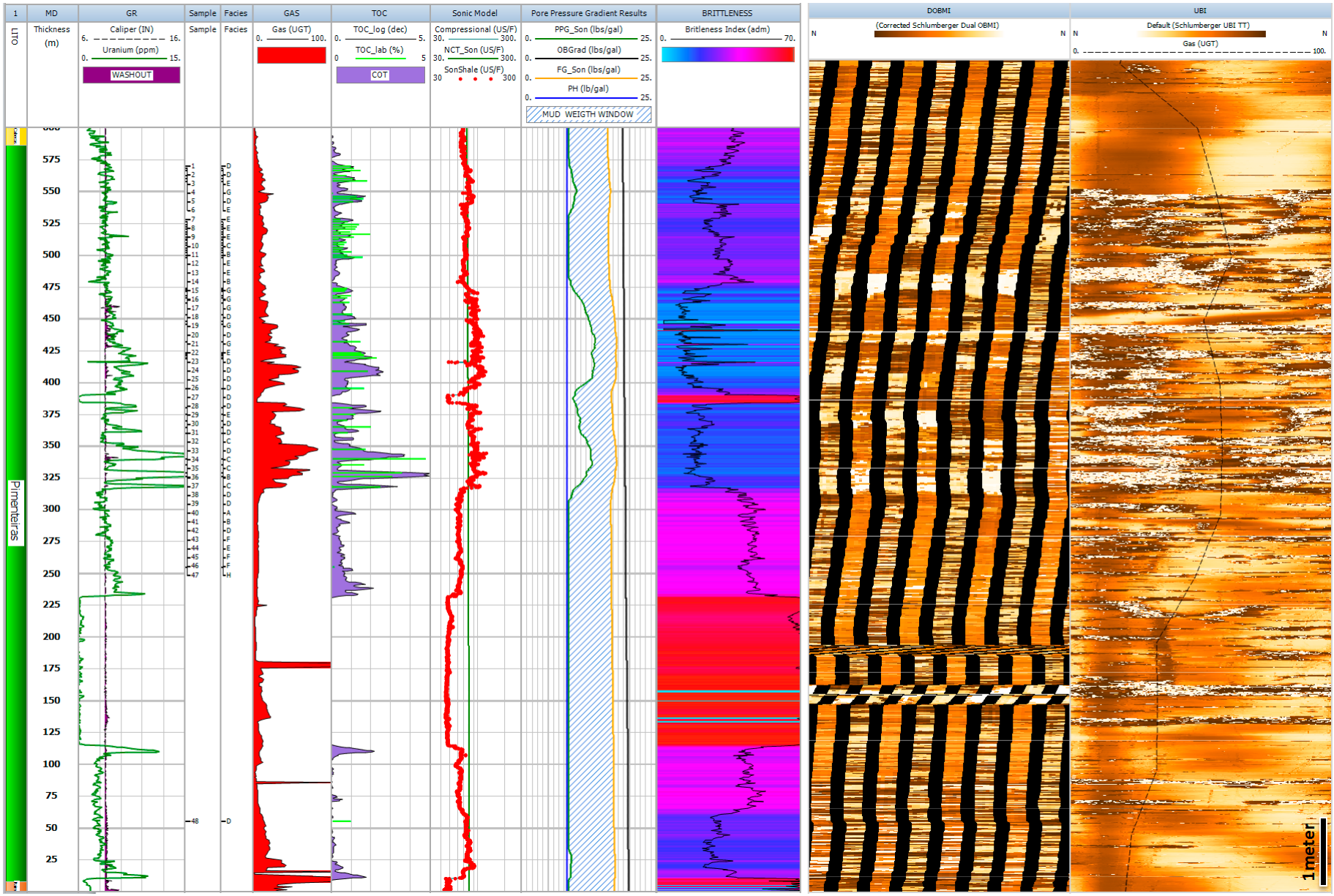

Figure 12. Composite log with Uranium content, caliper, sample number, sample facies, gas shows, sidewall core TOC measurement, log-derived TOC, resistivity, pore pressure gradients, and brittleness index. The two rightmost tracks are the resistivity and acoustic image logs. The relation between TOC, gas shows and overpressured zones suggests an effective shale gas system.

FACIES		Lithology	SEDIMENTARY STRUCTURES	TRACE FOSSILS	PROCESSES	INTERPRETATION	NMR POROSITY (%)	TOC (%)	EoD	Samples
A	Mss	Muddy-sandstone	Sharp tabular bedding, wave-cross laminated, micaceous, pyrite lags.	None	STORM WAVE RE-WORK (?)	Oxic environment with high energy.	7.0	0.8	Wave-influenced Delta Front	40
B	Msc	Muddy-sandstone couplet	Sharp tabular bedding, plane-parallel to ripple laminated, gutter cast, micaceous.	None	TURBIDITY CURRENT	Oxic environment with high energy.	5.3	2.0		11, 14, 36, 41
C	Smc	Sandy-mudstone couplet	Sharp tabular, plane-parallel to ripple laminated, gutter cast, micaceous.	None	TURBIDITY CURRENT	Suboxic environment with high energy.	5.3	2.0		10, 32, 34, 35, 37
D	Bmsc	Bioturbated sandy-mudstone couplets.	Burrowed bedded, concave-up lamina, gutter cast, fining-up, micaceous.	Planolites (Pl), Palaeophycus (Pa), Helminthopsis (He), Chondrites (Ch), Skolithos (Sk), Rhizocorallium (Rh).	TURBIDITY CURRENT	Oxic enviromnet with moderate to low energy.	4.7	1.1	Prodelta	1, 2, 5, 18, 20, 23, 24, 25, 26, 27, 28, 30, 31, 33, 38, 39, 42, 48
E	Lcs	Laminated Claystone to Siltstone	Faint sharp tabular bedded, plane parallel laminated, micaceous.	Meiofauna (?)	TURBIDITY CURRENT/BOTTOM CURRENT (?)	Oxic environment with low energy.	5.0	1.4		3, 6, 7, 8, 9, 12, 13, 22, 29, 44
F	Orm	Organic rich mudstone	Sharp lensoidal, plane parallel, pyrite lag, micaceous, starved ripples.	None	BOTTOM CURRENT	Anoxic environment with low energy	4.4	3.1	Upper Offshore	43, 45, 46
G	Cms	Chaotic muddy-sandstone	Burrowed bedded, concave-up lamina.	Planolites (Pl), Teichichnus (Te), Ophiomorpha (Op).	TURBIDITY CURRENT	Oxic enviromnet with moderate to high energy.	8.0	0.6	Transgressive Lag	4, 15, 16, 17, 19, 21
H	Hor	Silisiclastic Hornfels	Faint tabular bedding, wavy discontinuous lamination, nodules	None	CONTACT METAMORPHISM	Fe-rich high temperature low pressure metamorphism	-	-	Contact Metamorphism	47

Table 1. Identified microfacies and its interpretations.